

$(\alpha + \gamma_1)$ Complex phase formation in the Cu-10 mass% Al-6mass% Ag alloy

A. T. Adorno · R. A. G. Silva · T. M. Carvalho

ICTAC2008 Conference
© Akadémiai Kiadó, Budapest, Hungary 2009

Abstract In this work the $(\alpha + \gamma_1)$ complex phase formation reaction in the Cu-10mass% Al-6mass% Ag alloy was studied using Differential Scanning Calorimetry (DSC), Differential Thermodilatometry (DTD), X-ray diffractometry (XRD), Optical (OM) and Scanning Electron Microscopies (SEM). The results indicated the presence of two different processes, related to a change in the Ag diffusion route from the α matrix to the $(\alpha + \gamma_1)$ complex phase.

Keywords Martensite · Cu–Al–Ag alloys · Thermodilatometry · Non-isothermal kinetics

Introduction

When an alloy is aged in the martensitic state the reverse transformation finish temperature increases with ageing time to a saturated value, a phenomenon known as martensite stabilization. Martensitic stabilization processes are responsible for some anomalies that damage shape memory phenomena such as changes in the transformation temperature and others [1–5]. Cu–Al alloys containing 9–14 mass% of Al are among those showing a martensitic phase after rapid cooling from high temperatures. The heating of Cu–Al martensite phase at a constant temperature below the eutectoid transformation temperature (martensite ageing) leads to formation of the $(\alpha + \gamma_1)$ complex phase and the presence of an interposing order-disorder reaction, substitutional type parent and product phases, makes the

eutectoid reaction in this system distinguishable from other ones [6]. Literature results have been shown that during ageing of Cu–Al–Ag alloys the $(\alpha + \gamma_1)$ complex phase formation does not occur in the time and temperature range studied due to a martensite stabilization effect [7], but this phase transition process is detected by the continuous heating of the alloys [8]. This way the non-isothermal kinetics offers an opportunity to analyze the $(\alpha + \gamma_1)$ complex phase formation. In this work non-isothermal kinetics of the $(\alpha + \gamma_1)$ formation reaction in the Cu-10mass% Al-6mass% Ag alloy was studied using differential thermodilatometry (DTD), differential scanning calorimetry (DSC), X-ray diffractometry (XRD), optical (OM) and scanning electron microscopies (SEM).

Experimental procedure

Cu-10mass% Al-6mass% Ag alloy was prepared in an induction furnace under argon atmosphere using 99.97% copper, 99.95% aluminum and 99.98% silver as starting materials. Results from chemical analysis indicated a final composition very close to the nominal one. The samples were annealed for 120 h at 850 °C for homogenization. After this, one annealed sample was equilibrated at 850 °C for 1 h and then quenched in iced water to reach the maximum dissolution of Ag and martensite formation. After the heat treatments the samples were polished, etched and examined by scanning electron microscopy (SEM) using a JEOL JSM T330A electron microscope with a Noran energy dispersive X-ray (EDX) microanalyser and by optical microscopy (OM) using a Leica DMR optical microscope. The X-ray diffraction (XRD) patterns were obtained using a Siemens D5000 4B diffractometer, Cu K α radiation and solid (not powdered) samples. DSC curve

A. T. Adorno (✉) · R. A. G. Silva · T. M. Carvalho
Instituto de Química—Unesp, C. Postal 355, Araraquara,
SP 14801-970, Brazil
e-mail: atadorno@iq.unesp.br

was obtained using a TA instrument Q20, by using aluminum pan, nitrogen flux at about 50 mL min^{-1} and solid sample with diameter of 3.0 mm. Small cylinders of about 10 mm length and 5 mm diameter were used for thermodilatometry (TD) investigations, carried out with a Netzsch 402E electronic dilatometer with molybdenum pipe furnace and a protective gas atmosphere of nitrogen and hydrogen. The differential thermodilatometry and DSC curves were obtained using a graphic program.

Results and discussion

Figure 1 shows the DSC curve obtained at a heating rate of $10 \text{ }^\circ\text{C min}^{-1}$ for the sample quenched from $850 \text{ }^\circ\text{C}$ in iced water. In this curve the exothermic peak P_1 , at about $280 \text{ }^\circ\text{C}$, is an event related to the martensite ordering reaction [9]. The exothermic peak P_2 , at about $410 \text{ }^\circ\text{C}$ is associated with Ag precipitation reaction [10] while endothermic peak P_3 , at about $475 \text{ }^\circ\text{C}$ is due to the martensite decomposition reaction. This transition is a combination of two consecutive reactions: the $\beta_1'' \rightarrow \beta_1$ disordering reaction and the partial β_1 decomposition giving the $(\alpha + \gamma_1)$ complex phase. P_4 , at about $520 \text{ }^\circ\text{C}$ is an endothermic peak due to the transition $\beta_1 \rightarrow \beta$ from part of the β_1 phase remnant from the transformation at $475 \text{ }^\circ\text{C}$. Peak P_5 is ascribed to the α phase precipitation reaction. This reaction is related to the γ_1 phase formation, which decreases Al concentration and changes the chemical composition of the alloy, making easier the α phase precipitation reaction. The endothermic peak P_6 is due to the $(\alpha + \gamma_1) \rightarrow (\alpha + \beta)$ reaction. The X-ray diffraction patterns shown in Fig. 2 confirm the proposed transformations

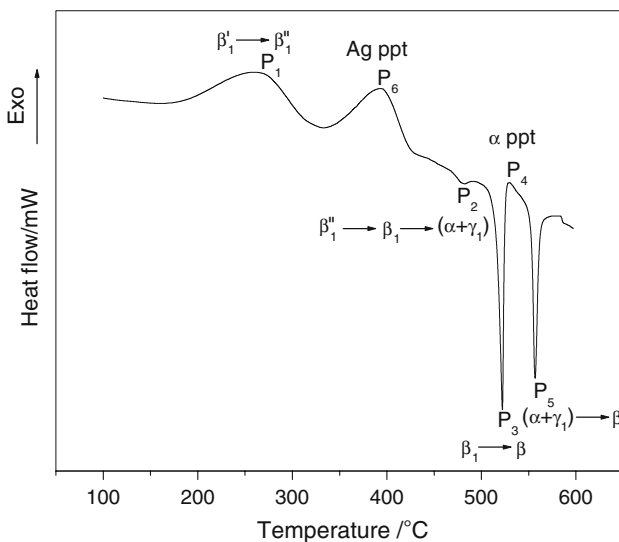


Fig. 1 DSC curve obtained for the Cu-10mass% Al-6mass% Ag alloy initially quenched

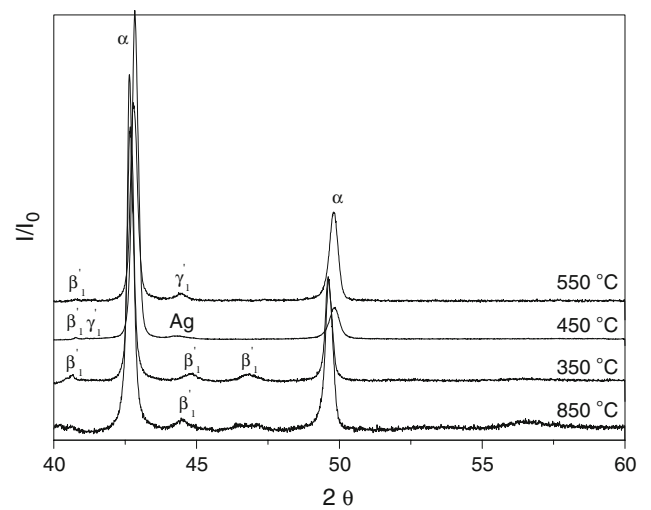


Fig. 2 X-ray patterns obtained for the Cu-10mass% Al-6mass% Ag alloy initially quenched

sequence, which is in good agreement with that found in the literature for hypoeutectoid Cu–Al alloys with additions of a third element [7, 8]. In the Cu-9 mass%Al and Cu-10 mass%Al alloys, the reverse martensitic transformation is observed at about $370 \text{ }^\circ\text{C}$ [11]. In the Cu-10mass% Al-6 mass% Ag alloy the presence of Ag shifted the reverse martensite temperature to higher values, suggesting that the presence of Ag disturbs the reaction mechanism.

The starting point of the DSC curves in Fig. 1 corresponds to the martensitic phase, as shown by the micrograph in Fig. 3a. It is known [12] that alloys with less than 10.8 mass%Al show the β' type martensitic phase and that for higher Al concentrations the observed martensitic phase is the β_1' . The micrograph in Fig. 3a shows the

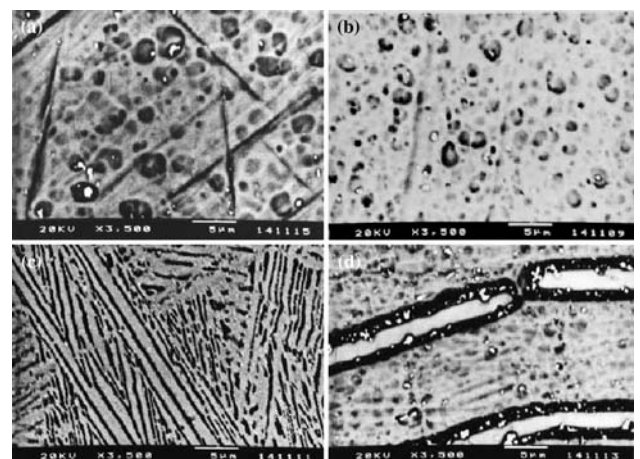


Fig. 3 SEM micrographs obtained for the Cu-10 mass% Al-6 mass% Ag alloy (a) quenched from $900 \text{ }^\circ\text{C}$ and then quenched from: (b) $300 \text{ }^\circ\text{C}$; (c) $500 \text{ }^\circ\text{C}$; (d) $600 \text{ }^\circ\text{C}$

characteristic structure of the β_1' martensitic phase, instead of the β_1' structure. It seems to indicate that the addition of 6mass%Ag to the Cu-10 mass%Al alloy shifts the equilibrium concentration to higher Al contents. From the DSC curve (Fig. 1) and X-ray diffraction patterns (Fig. 2) it was expected that the characteristic structure of the ($\alpha + \gamma_1$) phase could be observed at about 500 °C in Fig. 3c, but this is not the case. The ($\alpha + \gamma_1$) phase characteristic structure is shown in Fig. 4 for the annealed sample and its absence in Fig. 3 indicates that the amount of martensite decomposition up to 500 °C is very little and that the presence of Ag is disturbing the formation of the ($\alpha + \gamma_1$) phase.

The effect of Ag on the ($\alpha + \gamma_1$) phase formation was analyzed using non-isothermal kinetic data obtained from Differential Thermodilatometry (DTD) and the Kissinger method, considering that this reaction is diffusion controlled and only occurs on continuous heating [7].

Figure 5a shows the differential thermodilatometry curves (DTD) obtained at different heating rates for the Cu-10mass% Al-6mass% Ag alloy. In Fig. 5a it is possible to observe the presence of peak (P₁), at about 480 °C, which corresponds to a dilatation. This thermal effect occurs in the same temperature range of the β_1 decomposition reaction

observed in the DSC curve (peak P₂, Fig. 1) suggesting that this dilatation effect is due to the ($\alpha + \gamma_1$) complex phase formation. The sample dilatation is closely related to the presence of γ_1 phase, which has a complex body-centered cubic structure with a lattice parameter about three times that of the corresponding body-centered cubic metal [13]. The dilatation peaks in the DTD curves are shifted to higher temperatures with the increase of the heating rate, thus confirming that the ($\alpha + \gamma_1$) is a diffusive and thermally activated process.

The differential thermodilatometry peaks and characteristic temperatures shown in Table 1 served as a basis for determining the activation energies of the ($\alpha + \gamma_1$) complex phase formation from β_1 phase decomposition. These results were processed according to the method developed by Kissinger [14],

$$\ln \frac{\phi}{T_p^2} = C - \frac{E_a}{RT_p} \tag{1}$$

where ϕ is the heating rate, T_p the maximum on the DTD peak, E_a the activation energy, R the universal gas constant and C is the integration constants.

The linear relationship between $\ln \left[\frac{\phi}{T_p^2} \right]$ and $1000/T_p$ for the ($\alpha + \gamma_1$) formation reaction in the Cu-10mass% Al-6mass% Ag alloy is shown in Fig. 5b, where it is possible to observe the presence of two processes. The activation energy value obtained for lower temperatures (from 473 to 499 °C) was 267 kJ mol⁻¹ whereas that for higher temperatures (from 499 to 510 °C) was 97.0 kJ mol⁻¹.

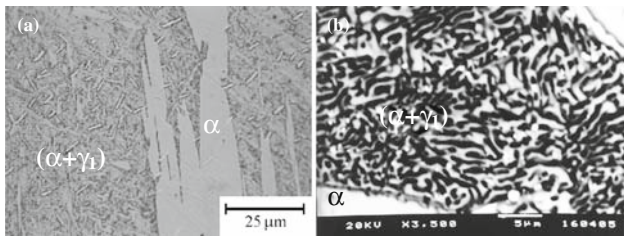
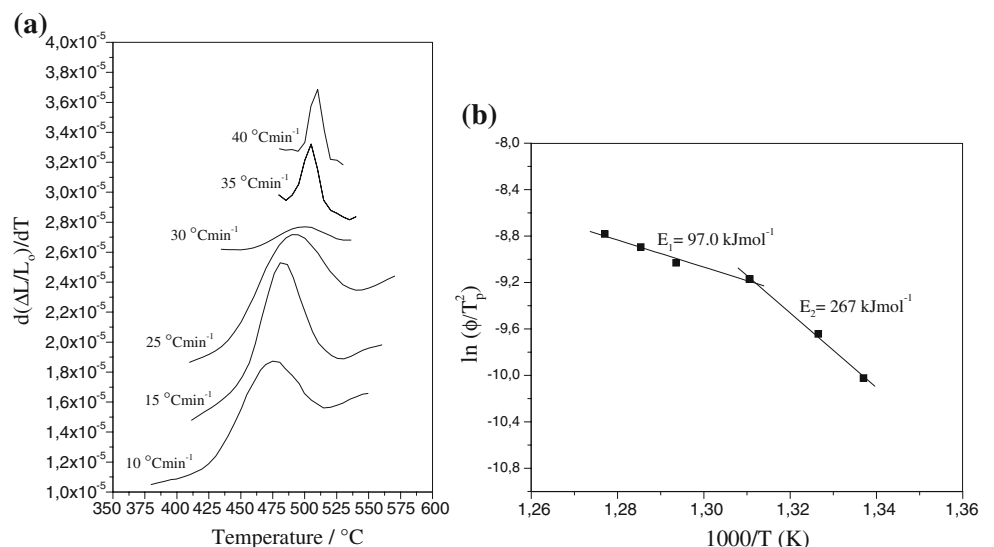


Fig. 4 (a) Optical micrograph and (b) SEM micrograph obtained for the Cu-10 mass% Al-6 mass% Ag alloy after annealing

Table 1 Temperature values obtained from Fig. 5a

| $\phi/^\circ\text{C min}^{-1}$ | 10 | 15 | 25 | 30 | 35 | 40 |
|--------------------------------|-----|-----|-----|-----|-----|-----|
| $T_p/^\circ\text{C}$ | 473 | 481 | 488 | 499 | 505 | 510 |

Fig. 5 (a) Differential thermodilatometry (DTD) curves obtained at different heating rates; (b) Plot of $\ln \left(\frac{\phi}{T_p^2} \right)$ versus $1000/T_p$



The activation energy value obtained for lower temperatures ($E_1 = 267 \text{ kJ mol}^{-1}$) is close to that obtained for the diffusion of Ag in the α -CuAl matrix ($E = 280 \text{ kJ mol}^{-1}$) and so, the process with activation energy $E_2 = 97.0 \text{ kJ mol}^{-1}$ corresponds to the $(\alpha + \gamma_1)$ phase formation. From Fig. 1 it is possible to observe that Ag precipitation occurs in the temperature range between 330 and 410 °C, just before the beginning of the $(\alpha + \gamma_1)$ phase formation (420–520 °C, Figs. 1 and 5a). After precipitation, with the increase of temperature part of the Ag atoms are re-dissolved into the matrix, a process that occurs before the $(\alpha + \gamma_1)$ formation reaction. As the temperature increases, the $(\alpha + \gamma_1)$ phase formation becomes the dominant step, due to its more complex structure, to the decrease in the Ag solute content and to the increase in the Ag diffusion rate into the $(\alpha + \gamma_1)$ phase. The γ_1 phase has an open bcc type structure and the diffusion coefficient is greater than in the fcc α phase [15].

Conclusions

Non-isothermal kinetic analysis of the $(\alpha + \gamma_1)$ formation reaction from differential thermodilatometry (DTD) data indicated the presence of two processes, one at lower temperatures attributed to Ag diffusion into the α matrix, and other at higher temperatures attributed to the $(\alpha + \gamma_1)$ phase formation. The presence of two different processes is related to a change in the Ag diffusion route from the α matrix to the $(\alpha + \gamma_1)$ complex phase.

Acknowledgements The authors thank the support of FAPESP (Project no. 2006/04718-0), CAPES and CNPq.

References

- Ahlers, M. In: Proceedings of the ICOMAT-86, The Japan Institute of Metals, Nara, Japan, 1996; p. 786–93.
- Auguet C, Isalgue A, Lovey FC, Pelegrina JL, Ruiz S, Torra V. Metastable effects on martensitic transformation in SMA Part III. Tentative temperature effects in a NiTi alloy. *J Therm Anal Calorim.* 2007;89:537–42.
- Sepulveda A, Muñoz R, Lovey FC, Auguet C, Isalgue A, Torra V. Metastable effects on martensitic transformation in SMA Part II. The grain growth effects in Cu–Al–Be alloy. *J Therm Anal Calorim.* 2007;89:101–7.
- Isalgue A, Torra V, Yawny A, Lovey FC. Metastable effects on martensitic transformation in SMA Part VI. The Clausius–Clapeyron relationship. *J Therm Anal Calorim.* 2008;91:991–8.
- Auguet C, Isalgue A, Lovey FC, Martorelli F, Torra V. Metastable effects on martensitic transformation in SMA part 4. Thermomechanical properties of CuAlBe and NiTi observations for dampers in family house. *J Therm Anal Calorim.* 2007;88(2):537–48.
- Kulkarni SD. Thermodynamics of martensitic and eutectoid transformations in the Cu–Al system. *Thermodynamique des transformations martensitiques et eutectoïde dans le système Cu–Al* Thermodynamik martensitischer und eutektoïder umwandlungen im system Cu–Al. *Acta Metall.* 1973;21(10):1461–9.
- Adorno AT, Silva RAG. Martensite aging kinetics in the Cu-10wt.%Al and Cu-10wt.%Al-10wt.%Ag alloys. *J Mater Sci.* 2008;43:1087–93.
- Adorno AT, Silva RAG. Thermal Behavior of the Cu-10% mass Al and Cu-10% mass Al-4% mass Ag Alloys. *J Therm Anal Calorim.* 2004;75:629–35.
- Kwarciać J, Bojarski Z, Morawiec H. Phase transformation in martensite of Cu-12.4%Al. *J Mater Sci.* 1986;21:788–92.
- Adorno AT, Guerreiro MR, Ribeiro CA, Guerreiro CTR. Influence of silver additions on the thermal behavior of the Cu-8 Mass% Al alloy. *J Therm Anal Calorim.* 2001;64:1141–6.
- Adorno AT, Guerreiro MR, Benedetti AV. Thermal behavior of Cu–Al alloys near the α -Cu₂Al solubility limit. *J Therm Anal Calorim.* 2001;65:221–9.
- Swann PR, Warlimont H. The electron metallography and crystallography of copper–aluminum martensites. *Acta Metall.* 1963;11:511–27.
- Smallman RE, Hume-Rothery W, Haworth CW. The structure of metals and alloys. London: The Institute of Metals; 1988.
- Kissinger HE. Reaction kinetics in differential thermal analysis. *Anal Chem.* 1957;29:1702–6.
- Ruzzante JE, Kurokawa S, García EA, Dymant F. Diffusion in the β/γ_2 interphase boundary of the Cu–Al system. *Acta Metall.* 1979;28:699–707.